Diagn Interv Radiol 2005; 11:35-40

ORIGINAL ARTICLE

Preoperative evaluation of renal anatomy and renal masses with helical CT, 3D-CT and 3D-CT angiography

Uğur Toprak, Aysun Erdoğan, Mutlu Gülbay, Mehmet Alp Karademir, Eşref Paşaoğlu, Ökkeş Emrah Akar

PURPOSE
The aim of this prospective study was to determine the efficacy of three-dimensional computed tomography (3D-CT) and three-dimensional computed tomographic angiography (3D-CTA) that were reconstructed by using the axial images of the multiphasic helical CT in the preoperative evaluation of renal masses and demonstration of renal anatomy.

MATERIALS AND METHODS
Twenty patients that were suspected of having renal masses upon initial physical examination and ultrasonographic evaluation were examined through multiphasic helical CT. Two authors executed CT evaluations. Axial images were first examined and then used to reconstruct 3D-CT and 3D- CTA images. Number, location and size of the renal masses and other findings were noted. Renal vascularization and relationships of the renal masses with the neighboring renal structures were further investigated with 3D-CT and 3D-CTA images.

RESULTS
Out of 20 patients, 13 had histopathologically proven renal cell carcinoma. The diagnoses of the remaining seven patients were xanthogranulomatous pyelonephritis, abscess, simple cyst, infected cyst, angiomyolipoma, oncocytoma and arteriovenous fistula. In the renal cell carcinoma group, 3 patients had stage I, 7 patients had stage II, and 3 patients had stage III disease. Sizes of renal cell carcinoma masses were between 23 mm to 60 mm (mean, 36 mm). Vascular invasion was shown in 2 renal cell carcinoma patients. Collecting system invasion was identified in 11 of 13 renal cell patients. These radiologic findings were confirmed with surgical specimens.

CONCLUSION
Three-dimensional CT and 3D-CTA are non-invasive, effective imaging techniques for the preoperative evaluation of renal masses.

Key words: • *computed tomography* • *three dimensional CT angiography* • *kidney* • *surgery*

From the Department of Radiodiagnostics (U.T. ✉), Ankara Numune Training and Research Hospital Sıhhiye, Ankara, Turkey.

Received 02 January 2004; first revision requested 02 June 2004; first revision received 10 October 2004; second revision requested 17 January 2005; second revision received 25 January 2005; accepted 28 January 2005.

The role of computed tomography (CT) in the evaluation of renal lesions is very well-known (1). CT is widely accepted as the preferred imaging technique for suspected renal tumors, and also has an important role in tumor staging. Benign renal processes, including cystic disease, renal infection, and benign tumors may simulate malign renal tumors, and could be defined correctly by CT (2). The improvements in CT technique and increased use of cross-sectional imaging have facilitated the detection of small or previously undiagnosed renal masses (3). Helical CT technology further improved renal imaging with decreasing volume-averaging artefacts, eliminating respiratory misregistration artefacts and allowing image acquisition during the peak intravenous contrast enhancement (4-7). Helical CT image acquisition has also led to improved data sets available for three-dimensional imaging (8-10).

To date, the major role of three-dimensional (3D) CT imaging for renal pathology has concentrated on the non-invasive evaluation of renal artery stenosis and other renal vascular abnormalities (11-13), but literature reveals a limited number of studies that describe the use of 3D-CT imaging and 3D-CT angiography (CTA) in renal mass evaluation (3, 8, 14).

The aim of this study was to investigate the efficacy of multiphasic helical CT, 3D-CT imaging and CTA in the demonstration of renal anatomy during the preoperative evaluation of renal masses.

Materials and methods

Twenty patients (16 females and 4 males) between the ages of 38-75 years (mean, 64 years) were involved in this prospective study. The patients had applied to physicians with such complaints as flank pain, hematuria, weight loss and fever, and all were initially evaluated with ultrasonography. The patients were suspected of having a renal mass based on ultrasonographic examination results. Thus, a computed tomographic examination was proposed for every single case.

Multiphasic helical CT scans were obtained using a Hitachi Radix Turbo scanner (Kashiwa, Chiba, Japan). No oral contrast agent was administered, because it interferes with volume rendering technique. Scanning parameters were as follows: 120 kVp, 175 mAs, and 1 revolution/s gantry rotation speed.

After obtaining scan projection radiograph, unenhanced CT was performed to localize the kidneys, identify calcifications and renal calculi, and demonstrate any fat within the lesion. A collimation of 5 mm, a table speed of 5 mm per revolution, and an image reconstruction interval of 5 mm were used.

For each study, 150 ml of contrast material was injected intravenously at 4 ml/sec through an antecubital vein. Arterial-phase images were obtained after a 20-second delay with a collimation of 3 mm, table speed

of 1 mm per revolution, and an image reconstruction interval of 1 mm. The arterial phase was used to depict the renal arteries, which is the most sensitive phase for the detection of multiple renal arteries and other possible arterial abnormalities.

Parenchymal-phase imaging was initiated approximately 240 seconds after the contrast material injection with a collimation of 3 mm, a table speed of 2 mm per revolution, and an image reconstruction interval of 2 mm. The parenchymal phase was used for lesion characterization and demonstrating the collecting system anatomy. In the arterial phase, small lesions may be overlooked in the unenhanced renal medulla and these lesions should be evaluated in the parenchymal phase more sensitively.

Thorax and the rest of the abdomen were scanned with the standard parameters for disease staging in patients with malignant masses.

All the axial images were thoroughly evaluated before the 3D reconstructions were performed; this is required because small vessels are easily overlooked on the 3D image if they are not identified first on the axial images. Additionally, in the axial images, the masses were evaluated for contour characteristics (regular or irregular), internal structure of the mass (homogeneous or heterogeneous), presence of calcifications and adipose components to determine their nature radiologically. Their attenuation values were compared to that of the renal cortex, and the degree of contrast enhancement was determined.

After the axial images were thoroughly examined, they were used to produce 3D images via embedded software of the CT equipment. Three-dimensional volume rendering method was preferred because it retained all data by summing the contributions from all the voxels along a line from any viewing angle through the axial images. Once the 3D reconstructions were achieved, two dimensional cut planes were applied to determine extensions of the masses.

Furthermore, tumor position and depth of extension were evaluated by using the cut planes. Both axial images and 3D reconstructions of the renal vessels were examined for possible tumoral invasion, thromboses and any other vascular abnormalities.

Deformation of the collecting system and mass surrounding the calyces or infundibula were considered as definitive invasion criteria. Compressed or flattened calyx and narrowed in-

Table 1. Number and dimensions of masses, extension of malignancy, and treatment features of renal cell carcinoma patients

Case	Diagnosis	Number of mass(es)	Dimensions (mm)	Extension of the malignant mass	Stage[a]	Treatment
1	Renal cell carcinoma	1	33x31	Perirenal fat	II	Partial nephrectomy
2	Renal cell carcinoma	1	32x31	Confined to one kidney	I	Partial nephrectomy
3	Renal cell carcinoma	1	34x37	Extension into renal vein	IIIA	Radical nephrectomy
4	Renal cell carcinoma	1	39x36	Perirenal fat	II	Partial nephrectomy
5	Renal cell carcinoma	1	27x33	Perirenal fat	II	Partial nephrectomy
6	Renal cell carcinoma	1	35x39	Perirenal fat	II	Partial nephrectomy
7	Renal cell carcinoma	1	36x38	Perirenal fat	II	Partial nephrectomy
8	Renal cell carcinoma Germ cell tumor	1 1	28x28 50x60	Perirenal fat	II	Radical nephrectomy
9	Renal cell carcinoma	1	47x57	Extension into renal artery and vein, IVC[b], regional lymph nodes	IIIC	Radical nephrectomy
10	Renal cell carcinoma	1	52x46	Regional lymph nodes	IIIB	Radical nephrectomy
11	Renal cell carcinoma Chronic pyelonephritis	1	29x36	Perirenal fat	II	Radical nephrectomy
12	Renal cell carcinoma	1	25x24	Confined to one kidney	I	Partial nephrectomy
13	Renal cell carcinoma	1	23x25	Confined to one kidney	I	Partial nephrectomy

[a] Robson stages of the malignant masses
[b] Inferior vena cava

Table 2. Diagnoses, number and dimensions of lesions and treatment features in patients with benign lesions

Case	Diagnosis	Number of mass(es)	Dimensions (mm)	Treatment
1	Abscess	1	26x29	Systemic antibiotic
2	Simple cyst	1	40x55	Aspiration-sclerotherapy
3	Infected cyst	1	65x70	Aspiration-sclerotherapy
4	Angiomyolipoma	1	20x14	Follow up
5	Arteriovenous fistula	2	22x22 25x25	Embolization
6	Oncocytoma	1	30x30	Partial nephrectomy
7	XGP[a]	1	20x10	Partial nephrectomy

[a] Xanthogranulomatous pyelonephritis

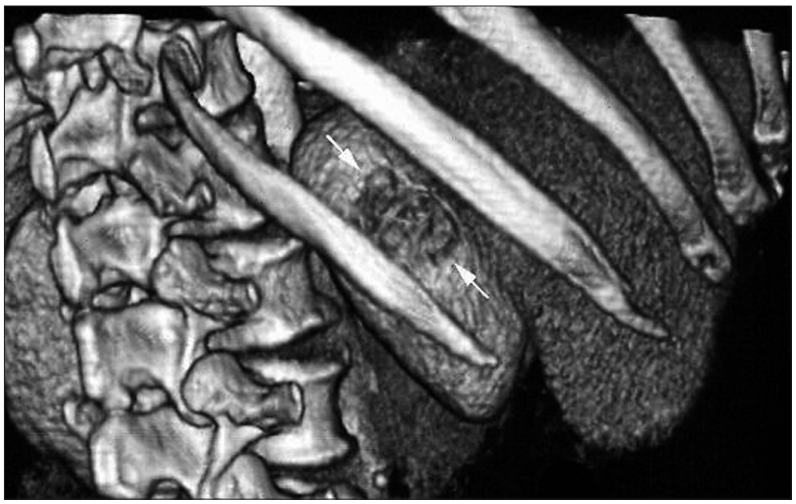

Figure 1. A 70-year-old male patient with renal cell carcinoma. Three-dimensional volume-rendered image shows both the location and the relationship of the low-attenuated tumor to the adjacent organs (spine, ribs and liver). Tumor *(arrows)* lies between the 11th and 12th rib levels.

Figure 2. A 70-year-old male patient with renal cell carcinoma. Three-dimensional volume-rendered image obtained with a cut plane in the oblique coronal orientation shows an interpolar region tumor with extension *(arrowheads)* to perirenal fat tissue.

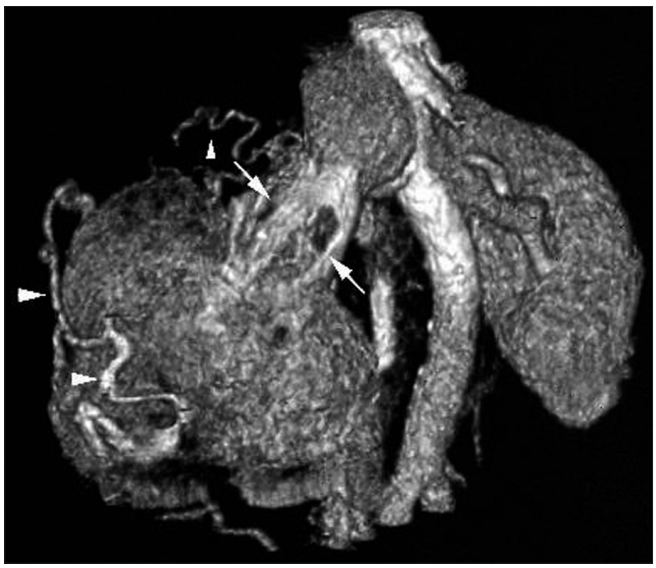

Figure 3. A 63-year-old female patient with renal cell carcinoma. Three-dimensional volume-rendered image shows widening of the right renal vein due to thrombosis *(arrows)*. Note the perirenal collateral vessels *(arrowheads)*.

fundibulum due to mass effect were considered suspicious findings for invasion.

Results

Out of 20 patients, 13 had histopathologically proven renal cell carcinoma. Diagnoses of the remaining 7 patients were as follows: xanthogranulomatous pyelonephritis, abscess, simple cyst, infected cyst, angiomyolipoma, oncocytoma and arteriovenous fistula (AVF). In the renal cell carcinoma group, 3 patients had stage I, 7 patients had stage II, and 3 patients had stage III disease (Tables 1 and 2). Sizes of renal cell carcinoma masses were between 23 mm to 60 mm (mean, 36 mm).

In the unenhanced examination, masses of AVF and oncocytoma were isodense with the renal cortex while all other masses were hypodense. One renal cell carcinoma had internal calcification. Adipose tissue component was only demonstrated in angiomyolipoma. Benign masses (n=7) were homogeneous and well-circumscribed whereas 11 of 13 renal cell carcinomas were heterogeneous and irregular in contour. All masses showed contrast enhancement except for the simple renal cyst. Five of the benign masses (angiomyolipoma, AVF, simple renal cyst, infected renal cyst and renal abscess cases) were definitely diagnosed with CT examination. All of the other renal lesions (focal xanthogranulomatous pyelonephritis, oncocytoma, germ cell tumor and renal cell carcinomas) were identified particularly after the surgical approach and histopathologic examination.

A second mass located at the renal hilus was identified in a patient with renal cortical mass. Histopathologically, these lesions were diagnosed as renal cell carcinoma and co-existing extragonadal germ cell tumor.

There were patchy hypodense areas with poor contrast enhancement in the renal cortex in a case with renal cell carcinoma which was suggestive of pyelonephritis with CT examination. Histopathologic specimen of this patient revealed findings of both renal cell carcinoma and chronic pyelonephritis.

Based on 3D images, the location of the kidney in relation to the lower ribs, the iliac crest, and the spine was determined to help the surgeon in defining the position of the surgical incision (Figure 1). Then, the locations of the lesions were noted. There were 2 lesions in the upper pole, 6 lesions in the interpolar region and 12 lesions in the lower pole. All the lesions had extensions to the renal medulla (Figure 2), except for the cortically located

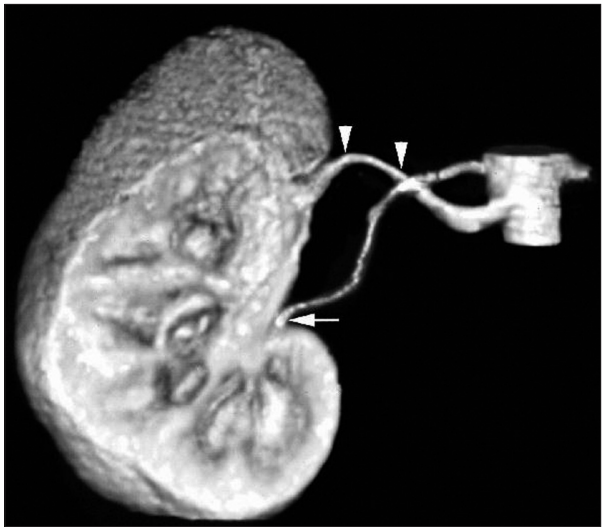

Figure 5. A 52-year-old female patient with renal cell carcinoma. Three-dimensional volume-rendered image shows an accessory renal artery *(arrow)* supplying the lower pole. The main renal artery is crossing behind the accessory renal artery *(arrowheads)*. A tumor is located in the upper pole (not shown in this view) of the kidney.

Figure 4. A 38-year-old female patient with arteriovenous fistula. Three-dimensional volume-rendered image obtained with cut plane in oblique sagittal orientation shows a densely enhancing vascular mass with feeding and draining vessels *(arrowheads)*. The relationship of the fistula with the left renal artery *(long arrows)* and vein *(short arrows)* is visible.

Figure 6. A 60-year-old male patient with renal cell carcinoma. Three-dimensional volume-rendered image obtained with cut plane in coronal orientation shows tumor *(open arrows)* distorting the lower pole calyces *(arrowheads)*. Displaced calyces at the superior border of the tumor can be seen *(arrows)*.

angiomyolipoma.

After the location of the lesions was noted, their possible extensions were searched. In two cases, there were vascular invasion accompanying the malignant lesions. In one case with a lesion located in the perihilar region, both renal artery and vein had been invaded by the lesion, and there was a thrombus in the inferior vena cava (IVC). Thrombus in the renal vein was seen in another case with a malignant lesion located at the midregion of the kidney (Figure 3). The results of the histopathologic evaluation of these two cases indicated renal cell carcinoma and vascular findings, which were confirmed pathologically. Perirenal collateral veins were noted in these two patients with renal vein invasion (Figure 3). However, in four patients with renal cell carcinoma, there were perirenal vessels, while there was no thrombosis in the renal vein or IVC.

Three of the patients with renal cell carcinoma had early venous contrast enhancement due to arteriovenous shunts within the lesion.

In this study, vascular involvement, which was only encountered in malignant processes, was not a finding. There were partial thrombi in renal artery and total thrombosis in renal vein in one case with an infected renal cyst.

Ultrasonographic examination of the patient with simple renal cyst showed intensive internal debris that led to suspicions of intramural solid component; thus, CT evaluation was proposed. In addition, the definite diagnosis of the renal cyst did not include intramural solid component, and 3D-CT and CTA revealed that the cyst was compressing the segmental renal artery. Interestingly, this patient also suffered from hypertension. Thus, the latter finding explained the patient's condition.

The patient with AVF had a history of a percutaneous renal biopsy with the diagnosis of glomerulonephritis ten years previously. It was demonstrated by its feeding and draining vessels with an enlarged renal artery and vein through 3D-CT imaging and CTA (Figure 4). It was concluded that the AVF developed as a complication of the biopsy procedure. This patient's angiography was per-

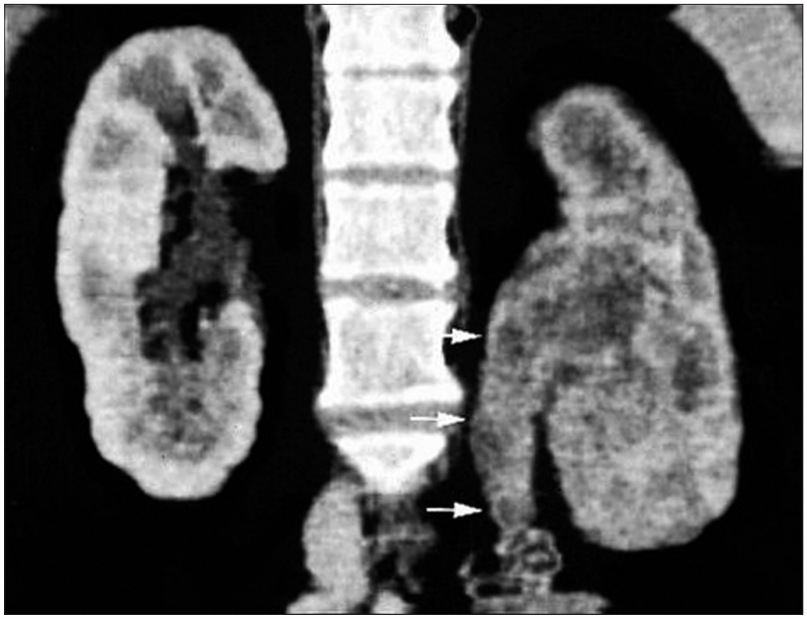

Figure 7. A 60-year-old female patient with renal cell carcinoma. Three-dimensional volume-rendered image shows a central tumor with ureteral extension *(arrows)*.

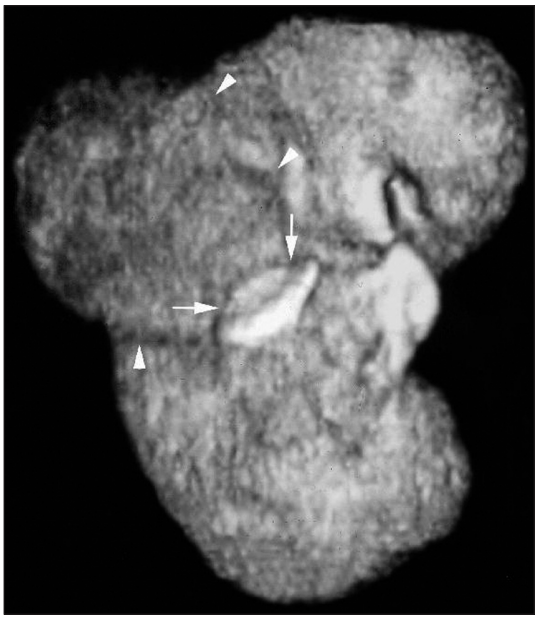

Figure 8. A 60-year-old female patient with renal cell carcinoma. Three-dimensional volume-rendered image shows a tumor arising from the lateral part of the kidney *(arrowheads)*. Note the flattening and compression of the middle calyx *(arrows)*.

formed during the embolization treatment and confirmed the CT findings.

A duplicated renal artery, an accessory renal artery, a retroaortic renal vein and an aneurysm of the celiac trunk were diagnosed in different renal cell carcinoma patients as co-incidental vascular findings and were confirmed surgically (Figure 5).

Eleven of 13 patients with renal cell carcinoma had a diagnosis of the invasion of pelvicalyceal system on CT examination, and this was confirmed intraoperatively (Figure 6). A proximal ureteral invasion was also shown in two of these eleven patients (Figure 7).

There were two cases with a compressed and flattened calyx. Although it was described as a suspicious criterion of invasion in our radiologic interpretation, calyceal invasion was observed both surgically and histopathologically in one of these patients (Figure 8). In the other case, compressed calyx was the only manifestation, and there was no evidence of the collecting system invasion intraoperatively and histopathologically.

There were three patients with a benign disease process extending to the medulla. In two of these patients (one oncocytoma and one simple renal cyst patient) collecting systems were completely normal. The CT examination of the patient with xanthogranulomatous pyelonephritis revealed a narrowed infundibulum. Surgical intervention (partial nephrectomy) was performed on both oncocytoma and xanthogranulomatous pyelonephritis patients, and surgical results confirmed the radiological findings.

Partial nephrectomy was performed on 10 patients (eight with renal cell carcinoma, one with oncocytoma, and one with xanthogranulomatous pyelonephritis). Radical nephrectomy was performed on five patients with renal cell carcinoma. Simple renal cyst and infected renal cyst cases were treated by percutaneous aspiration and sclerotherapy (absolute alcohol was used as the sclerosing agent). Percutaneous aspiration and sclerotherapy of the cyst caused a significant improvement of the hypertension of the patient with simple renal cyst. Systemic antibiotic therapy was given to the patient with infected renal cyst after the percutaneous aspiration and sclerotherapy procedure. Renal abscess was treated with intravenous antibiotics. The patient with AVF underwent embolization procedure. Regular follow-ups with CT were recommended for the case with angiomyolipoma.

Discussion

Complete and extensive information about the renal mass is needed by the clinician to determine the appropriate treatment modality. That means extensions of the mass as well as relations with adjacent structures such as vessels and the ureter. The latter one is especially important for benign masses because they may lead to compression of renal vessels or the ureter rather than a true invasion. Furthermore, renal vascularization shows variation and must be clarified before any surgical approach.

Perirenal collateral veins are usually observed in patients who have renal vein thrombosis. In a study by Zeman et al., perirenal collateral vascularization was identified in 12 of 18 renal cell cancer patients with renal vein invasion (15). In our study, perirenal collateral veins were identified in two cases with renal vein invasion. However, in four patients, perirenal vascularizations were shown in the absence of renal vein and IVC thrombosis. Unfortunately, it could not be determined whether these were dilated capsular veins or collateral vessels through CT evaluation.

In addition to primary tumors, variations like renal artery duplications, accessory renal artery, retroaortic renal vein and abnormalities such as aneurysm of the celiac trunk were also demonstrated. Thus, without performing

an angiography, a single imaging modality performed preoperatively could provide sufficient information about the accompanying vascular abnormalities, thus granting the opportunity to minimize the unexpected hemorrhagic complications associated with vascular variations.

In the patient with co-existent renal cell carcinoma and extragonadal germ cell tumor, it was demonstrated that the germ cell tumor was surrounding and displacing the renal vasculature and the IVC. Surgical approach was planned by considering this finding. Adequate information about the tumor and its vascular neighbors guided the surgeon during planning the surgical procedure. Additionally, preoperative demonstration of the accessory vascular structures provided valuable help during the excision of the mass. There was no bleeding complication during the surgical interventions reported in our patient group.

Depiction of the relationships of the tumor to adjacent calyces allows the surgeon to anticipate extension into the collecting system and minimizes postoperative complications such as a urinary fistula or urinoma (8). The findings of eleven patients with renal cell cancer met the collecting system invasion criteria of this study (deformity of the collecting system and mass surrounding the calyces and infundibula). Additionally, proximal ureteral invasion was seen in two patients. All suggested invasions were proven surgically. Thus, these findings should be accepted as reliable criteria in determining the collecting system invasion. Compressed or flattened calyces and narrowed infundibula due to mass effect were considered suspicious findings of invasion in our study, and there were two instances of renal cell carcinoma meeting these criteria. Collecting system invasion of the tumoral mass was shown in only one of these cases. Thus, those criteria should be considered suspicious in terms of invasion, and it should be kept in mind that these findings never exclude the possibility of collecting system involvement.

In our study group, all radiologically detected tumoral masses were confirmed with surgical interventions. However, it must be remembered that renal pseudotumors can be caused by respiratory misregistration. Other factors which cause the suboptimal image quality are under-filling of the pelvicalyceal system with contrast medium, hydronephrosis obliterating the calyceal detail and motion artifacts (8, 16). Thus, when such confusing appearances exist, careful interpretation is needed to avoid misdiagnosis.

Appropriate helical CT protocols and volume rendering techniques result in 3D images of high quality. In our study, we used a thin collimation and reconstruction index. Consequently, problems such as stepping artifacts were minimized. Three-dimensional CT imaging and CTA have many advantages in the evaluation of renal masses compared to routine renal CT protocols. However, it should be remembered that both 3D-CT and CTA procedures depend on axial images, and all of these procedures complement each other for a reliable evaluation. Three-dimensional applications provide rotation of the kidney image in different positions and facilitate obtaining cut planes; hence, the relationship of the mass with the renal tissue and adjacent organs is demonstrated better and the mass is defined to its finest detail. In some occasions, definitive diagnosis of vascular or pelvicalyceal invasion depending on 2D axial images is very difficult. Three-dimensional CT imaging and CTA provides better images in the determination of the vascular and collecting system invasion. Identification of the relationship of the mass with adjacent vessels both affects the treatment procedure and decreases possible operative complications. Additionally, determining the collecting system invasion has important contributions to the treatment protocol both in benign and malignant masses.

In conclusion, 3D-CT by itself provides valuable data about the nature and regional features of the mass, and it can be used as part of a single-step study procedure when combined with the other CT procedures for renal malignancy staging.

References

1. Bluemke DA, Fishman EK. Spiral CT of the abdomen: clinical applications. Crit Rev Diagn Imaging 1993; 34:103-157.
2. Bosniak MA. The small (less than or equal to 3.0 cm) renal parenchymal tumor: detection, diagnosis, and controversies. Radiology 1991; 179:307-317.
3. Smith PA, Marshall FF, Urban BA, Heath DG, Fishman EK. Three-dimensional CT stereoscopic visualization of renal masses: impact on diagnosis and patient treatment. AJR Am J Roentgenol 1997; 169: 1331-1334.
4. Wyatt SH, Urban BA, Fishman EK. Spiral CT evaluation of kidneys. In: Fishman EK, Jeffrey RB, eds. Spiral CT: Principles, Techniques and Clinical Applications. Philadelphia: Lippincott-Raven, 1996; 87-107.
5. Cohan RH, Sherman LS, Korobkin M, Bass JC, Francis IR. Renal masses: assessment of corticomedullary-phase and nephrographic-phase CT scans. Radiology 1995; 196:445-451.
6. Kalender WA, Seissler W, Klotz E, Vock P. Spiral volumetric CT with single-breath-hold technique, continuous transport, and continuous scanner rotation. Radiology 1990; 176:181-183.
7. Curry NS. Small renal masses (lesions smaller than 3 cm): imaging evaluation and management. AJR Am J Roentgenol 1995; 164:355-362.
8. Coll DM, Herts BR, Davros WJ, Uzzo RG, Novick AC. Preoperative use of 3D volume rendering to demonstrate renal tumors and renal anatomy. Radiographics 2000; 20:431-438.
9. Fishman EK, Magid D, Ney DR, Chaney EL, Pizer SM, Rosenman JG, Levin DN, Vannier MW, Kuhlman JE, Robertson DD. Three-dimensional imaging. Radiology 1991; 181:321-337.
10. Johnson PT, Heath DG, Bliss DF, Cabral B, Fishman EK. Three-dimensional CT: real-time interactive volume rendering. AJR Am J Roentgenol 1996; 167:581-583.
11. Kuszyk BS, Heath DG, Ney DR, Bluemke DA, Urban BA, Chambers TP, Fishman EK. CT angiography with volume rendering: imaging findings. AJR Am J Roentgenol 1995; 165:445-448.
12. Rubin GD, Dake MD, Semba CP. Current status of three-dimensional spiral CT scanning for imaging the vasculature. Radiol Clin North Am 1995; 33:51-70.
13. Rubin GD, Dake MD, Napel S, Jeffrey RB Jr, McDonnell CH, Sommer FG, Wexler L, Williams DM. Spiral CT of renal artery stenosis: comparison of three-dimensional rendering techniques. Radiology 1994; 190:181-189.
14. Chernoff DM, Silverman SG, Kikinis R, Adams DF, Seltzer SE, Richie JP, Loughlin KR. Three-dimensional imaging and display of renal tumors using spiral CT: a potential aid to partial nephrectomy. Urology 1994; 43:125-129.
15. Zeman RK, Cronan JJ, Rosenfield AT, Lynch JH, Jaffe MH, Clark LR. Renal cell carcinoma: dynamic thin-section CT assessment of vascular invasion and tumor vascularity. Radiology 1988; 167:393-396.
16. Heyns CF, van Gelderen WF. Three-dimensional computed tomographic imaging of the pelvicalyceal system: analysis of factors influencing image quality. Eur Urol 1992; 22:298-302.